OPEN ACCESS

ARTICLE

Journal homepage: www.the-innovation.org/energy-use

Energy Use

INNOVATION PRESS

Energy Use 2 (2025):100027

Contents lists available at INNOVATION PRESS

Charging Guidance Strategy for Electric Ride-Hailing Vehicles Oriented Towards Building Energy Sharing

Lei Gan,[1,*] Zhipeng Jia,[1] Le Bu,[1] Yangyi Hu,[1] Kun Yu,[1] Yubo Yuan,[2] Guiqing Feng,[3,*] Mei Liao,[3] Hong Liu,[3] and Giulia Taromboli[4]

*Correspondence: leigan@hhu.edu.cn(L.G.); cforgetit@163.com (G.F.)

Received: November 20, 2025; Accepted: December 21, 2025; Published Online: December 24, 2025; https://doi.org/10.59717/ipj.energy-use.2025.100027

GRAPHICAL ABSTRACT

PUBLIC SUMMARY

- Proposes a framework combining electric ride-hailing vehicle (ERV) mobility sharing with building energy sharing demand to promote vehicle-to-building(V2B) interaction.
- A two-stage strategy oriented towards building energy sharing to guide spatial distribution of ERV charging loads.
- Pre-charging guidance matches the final car-hailing orders for ERVs triggered range alerts, considering the region of building energy sharing requirement.
- Guidance strategy recommends building charging piles that maximizes charging satisfaction for ERV drivers.

ARTICLE

OPEN ACCESS

Journal homepage: www.the-innovation.org/energy-use

Energy Use

INNOVATION PRESS

Energy Use 2 (2025):100027

Contents lists available at INNOVATION PRESS

Charging Guidance Strategy for Electric Ride-Hailing Vehicles Oriented Towards Building Energy Sharing

Lei Gan,[1,*] Zhipeng Jia,[1] Le Bu,[1] Yangyi Hu,[1] Kun Yu,[1] Yubo Yuan,[2] Guiqing Feng,[3,*] Mei Liao,[3] Hong Liu,[3] and Giulia Taromboli[4]

[1]School of Electrical and Power Engineering, Hohai University, Nanjing 210024, China

[2]State Grid Jiangsu Electric Power Co., Ltd., Nanjing 211106, China

[3]SEC (Shenzhen) Innovation & Technology Co., Ltd., Shenzhen 518000, China

[4]Department of Energy, Politecnico di Milano, Milano 20133, Italy

*Correspondence: leigan@hhu.edu.cn(L.G.); cforgetit@163.com (G.F.)

Received: November 20, 2025; Accepted: December 21, 2025; Published Online: December 24, 2025; https://doi.org/10.59717/ipj.energy-use.2025.100027

Citation: Gan L., Jia Z., Bu L., et al. (2025). Charging Guidance Strategy for Electric Ride-Hailing Vehicles Oriented Towards Building Energy Sharing. *Energy Use* 1:100027.

With the characteristics of spatial-temporal flexibility, the charging load of electric vehicles can provide excellent flexibility for the low-carbon and economical operation of buildings, via implementing rational charging guidance strategies. Focusing on the electric ride-hailing vehicle (ERV) group, a charging guidance strategy for ERVs is established oriented towards building energy sharing, accounting for the influence on spatial distribution of charging loads caused by online car-hailing order matching. First, combining ERV mobility sharing with building energy sharing demand together, an urban mobility-energy sharing service framework is constructed and illustrated with the integration of information, energy, and value flows. Then, considering the spatial effect of mobility orders on the following charging behavior, a two-stage guidance strategy of ERVs is proposed. The first stage deals with a pre-charging guidance problem with final car-hailing order matching for ERVs triggered range alerts considering the region of building energy sharing requirement. Subsequently, in the second stage, an optimal charging station recommendation strategy is proposed to meet the refined energy sharing demand of the buildings nearby, considering ERVs' charging decision-making behavior. Simulation results verify that the proposed method successfully creates a synergistic interaction between ERV charging loads and building energy sharing, with seamlessly improving the charging experience for ERV drivers.

INTRODUCTION

Research background

Building operational energy consumption accounts for 30% of the world's total energy end-uses, and its related carbon emissions account for 26% of global energy sector emissions.[1] These figures underscore the imperative to transition building energy systems toward green, low-carbon development[2-4] and to advance building electrification.[5,6] While, with the integration of distributed renewable energy and the rising demand for uncertain multi-energy loads, building energy management (BEM) faces significant challenges due to volatile price and carbon-containing factor of external power supply. In this context, the energy sharing[7,8] mechanism offers a novel solution to mitigate power supply-demand imbalances in building,[9,10] as well as enhancing the flexible adjustment capability[11,12] and operational efficiency[13] of building energy system. With this mechanism, electric vehicles (EVs) become a kind of promising medium to supply spatial and temporal flexible load resources to participate in BEM through charging-price guidance strategies.[14]

The past decade has witnessed a remarkable surge in the global EV market. With sales exceeding 17 million units in 2024 and projections indicating a global stock of hundreds of millions by 2030,[15] the ecosystem is rapidly evolving. Meanwhile, with the thriving sharing services,[16,17] the number of electric ride-hailing vehicles (ERVs)[18-20] is becoming non-negligible. ERVs, characterized by prolonged operational duration and frequent charging patterns, are regarded as pivotal assets for coordinated charging management within integrated power-transportation networks.[21-23] Similarly, their potential as interactive resources with building energy systems presents significant opportunities for enhancing the flexibility and low-carbon operation of urban buildings. Distinct from private vehicles, ERVs' operational data are consolidated through ride-hailing platforms, and their routing is predominantly order-driven. By integrating ERVs' charging demands with urban buildings' energy sharing needs on ride-hailing platforms, trip assignments can be coordinated with charging schedules, guiding vehicle-to-building (V2B) interactions and fostering low-carbon synergy between electrified transportation and buildings.

Existing work and research objective

Currently, EVs are widely utilized in vehicle-to-grid (V2G) and V2B interactions[24] due to their ability to regulate spatially and temporally variable electrical loads. Existing studies on EV charging load guidance strategies can be divided into two categories: time-dimensional guidance and space-dimensional guidance. Temporal guidance primarily focuses on optimizing charging schedules, leveraging the flexible load characteristics of EVs to enhance grid operational economy and security, such as promoting the local consumption of new energy,[25] improving the voltage of the distribution network,[26] and reducing the peak-valley load difference.[27] However, this approach requires significant temporal flexibility from EVs, making it difficult to apply to ERVs, which rely on fast charging and have the characteristic of uninterrupted charging loads in time.

In recent years, growing scholarly attention has been directed toward space-dimensional charging guidance strategies, which mainly covering three areas: charging path optimization,[28] dynamic charging navigation[29-31] and charging station recommendation.[32] Su et al.[29] introduced a multi-agent deep reinforcement learning algorithm by integrating modeling of three-party information from transportation networks, charging stations (CSs), and drivers, offering a new paradigm for charging navigation. Based on a hierarchical cyber-physical system, Tao et al.[30] employed distributed crowd-sensing technology to achieve fast CS assignment and charging navigation to EVs. To address the issue of distribution network voltage violation, Sun et al.[31] proposed a three-layer hierarchical voltage control strategy with customized charging navigation in the second layer, establishing a charging decision-making model covering six drivers' preference modes. Habbal et al.[32] integrated user preferences with multi-attribute decision-making theory to propose a novel CS recommendation scheme, providing users with accurate and personalized charging suggestions. These studies focus on general EVs, not available to the order-oriented feature of ERVs, whose routes are highly dependent on the spatial distribution of real-time mobility orders.

More critically, there is an inherent time conflict between charging behaviors of ERVs and their order-accepting behaviors. Due to their unique operational characteristics, scholars have conducted a series of studies on ERV charging guidance. Yi et al.[33] proposed a comprehensive scheduling and charging management framework for autonomous electric ride-hailing fleets to improve transportation system operational and energy efficiency via centralized optimization. To address centralized scheduling defects, Wang et al.[34] used a multi-agent reinforcement learning framework to optimize urban ERVs' daily operations, covering scheduling, charging, and order response. Li et al.[35] integrated charging and order-accepting decisions-making into a Markov decision-making process, developing a two-stage heuristic coordinated reinforcement learning method that outperforms traditional approaches in driver income, passenger experience, and CS utilization. Li et al.[36] first integrated stochastic guidance, matching, and charging decision-making into a data-driven stochastic optimization framework. Zhong et al.[37] constructed a charging navigation method to provide optimal charging period and path to balance the load of CSs, divert traffic flow, and improve the operating income of electric taxis. Ni et al.[38] jointly modeled idle electric taxi charging scheduling and taxi-calling task assignment, innovatively proposing a task allocation framework that provides a reliable solution for electric taxi-hailing platform scheduling. While, the combined time and space sequence modeling of ERVs still requires further research to support mobility-order matching and charging recommendation.

As for the interaction between EVs and buildings, existing researches have shown that EV charging loads can participate in building demand-side management, thereby enhancing the local consumption of renewable energy, reducing building energy costs, and lowering carbon emissions. Patankar et al.[39] developed a scalable LSTM model to predict the charging and discharging power of EVs to support EV participation in BEMS. Dai et al.[40] established a real-world dataset encompassing different CSs, revealing the inherent behavioral and energy-use coupling between electric vehicles and buildings. This provides data support for EV participation in BEMS. However, it lacks of the research on the interaction of ERVs and building, collaboratively considering mobility sharing and energy sharing.

In summary, existing studies mainly concentrated on the overall benefit optimization of ERV fleet operators, considering passenger matching, vehicle scheduling, and charging guidance jointly. Few have considered the last mobility order's guiding role in the spatial distribution of charging load oriented to buildings' energy sharing requirement. When the state of charge (SOC) is close to the range anxiety threshold of drivers, ERV charging behavior can be effectively guided by a consecutive decision-making framework, with passenger mobility order matching followed by CS selection. Additionally, charging queuing time, a key factor affecting charging behavior, requires more refined calculation by a dynamic CS queue model considering multi-vehicle competition. Thus, a two-stage charging guidance strategy for ERVs is proposed here, based on the establishment of an urban mobility-energy combined sharing service framework. The main contributions are as follows:

1) Construct an urban mobility-energy sharing service framework based on the existing ride-hailing platform, and specifically elaborate on the information-energy-value flow (3-Flow) interaction mode and operation time sequence of the sharing service modules.

2) Propose an ERV charging pre-guidance mechanism that embeds mobility service chains into charging behavior guidance. By guiding the last order of ERVs, the spatial distribution of charging demand is dispersed, further improving the charging experience for ERVs.

3) Introduce an optimal CS recommendation system based on real-time information, achieving process linkage with pre-charging guidance (PCG) and providing an effective regulation means for participating in building energy sharing.

MATERIALS AND METHODS

Urban mobility-energy sharing service framework

Combined sharing service framework. Driven by the dual demands of guiding the charging behavior of ERV and optimizing BEM, this paper proposes an urban combined mobility-energy sharing service framework. The core function of existing car-hailing platforms is passenger mobility order matching with ERVs. Building upon this, our framework integrates charging guidance function into current platform. Note that the integrated charging guidance function include two key services for ERVs: PCG and CS recommendation, to promote energy sharing between ERVs and buildings. Thus, the proposed framework can be operated with the following four functional modules.

(1) Mobility order matching

A delayed centralized dispatching strategy is employed to match ERVs with passenger mobility demands. This strategy achieves an optimal matching by synthesizing real-time mobility data (e.g., origins, destinations, time windows), ERV status information (e.g., location, state of charge, service status), while ensuring all constraints on user service quality are met.

(2) Pre-charging guidance

The range anxieties of ERV drivers can be preset to the platform, or can be observed from their usual charging habits by the platform. When the real-time ERVs' SOC approximate the thresholds, they are triggered to start the PCG stage by the platform. In this stage, the platform can make one last mobility order matching for each of these ERVs before recharge. Different from the normal mobility order matching, the mobility order matching here at PCG stage combined the mobility order and the next stage of CS recommendation together by taking the regional charging prices of buildings into account. Based on the discrete event simulation method, the platform simulates ERV drivers' charging selection behavior and its spatiotemporal distribution through the coupled optimization of mobility orders and charging decisions, ultimately screening mobility orders that maximize charging satisfaction. This PCG stage can effectively disperse the spatial distribution of charging demand by using mobility orders, thereby improving the charging experience of ERV drivers, as well as considering buildings' energy sharing requirement reflected by their charging price.

(3) CS recommendation

Upon completing the final mobility order assigned in PCG stage, an ERV needs a suitable CS recommended to meet its charging demand. To overcome drivers' limited capacity for information processing, the platform can recommend several stations according to their charging satisfaction. The recommendation synthesizes three key factors: building-released charging prices, driving times derived from real-time traffic, and charging waiting times estimated from dynamic station queues. In contrast to the PCG stage, which relies on simulation to forecast behavior, critical uncertainties, like traffic conditions and charger availability, now resolve into determinate ranges as the vehicle approaches its charging event. Leveraging these high-confidence and multi-source data, the platform generates a globally optimal CS selection for the ERV.

(4) CS information update

To realize the functions of PCG and optimal CS recommendation, the platform not only needs to integrate mobility order information and ERV status information, but also needs to update and process multi-dimensional data of regional CSs, including the charging piles of energy-sharing buildings. The information that needs to be updated mainly includes the real-time charging prices, charging queues, geographic locations of idle charging piles.

Regarding the above four major modules, mobility order matching mainly realizes the mobility sharing service of the platform, while PCG and optimal CS recommendation form a two-stage coupled charging guidance method for ERVs to assist in completing the buildings' energy sharing service of the platform. CS information collection and update provides information support for the energy sharing service. Based on these two services of mobility sharing and energy sharing, the platform can not only efficiently match passengers' mobility orders, but also improve the charging experience of ERV drivers, and address the BEM problems with energy sharing.

The information-energy-value flow interaction mode. The 3-Flow interaction mode of the mobility sharing and the energy sharing service is specified as follows.

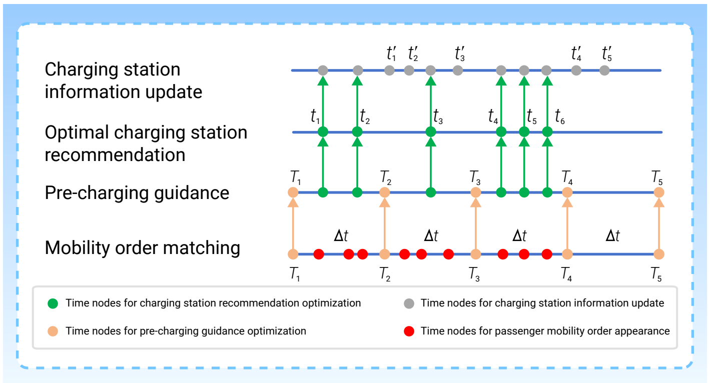

Figure 1. Module operation sequence of mobility-energy sharing service

(1) 3-Flow interaction mode of the mobility sharing service

Passengers send mobility requests and transmit relevant information to the platform. The platform matches suitable ERVs for passengers by collecting real-time location and SOC status of ERVs, and feeds back the matched vehicles information to the passengers. ERVs pick up and drop off passengers in accordance with the dispatch instructions from the platform to complete mobility orders, and then passengers pay service fees to the ERVs to complete value transmission. Finally, the platform deducts platform service fees from each mobility order, realizing value transmission from ERVs to the platform.

(2) The 3-Flow interaction mode of the energy sharing service

When the SOC status of an ERV is close to the range anxiety threshold, a PCG request is triggered by the platform automatically. At this time, the platform starts the mobility order matching for PCG, based on the updated CS information of buildings, the SOC status of ERVs, and the real-time travel request of passengers. Once PCG is finished, i.e. the last mobility order is completed, the CS recommendation service begins by the platform for the ERV.

Thus, the energy sharing service is mainly divided into two stages: in the first stage, the matching of the last mobility order is completed before charging, on the basis of simulating the charging selection behavior of ERVs. The 3-Flow interaction mode in this stage is similar to that of normal mobility sharing service, but additionally considers the regional buildings' energy-sharing charging price information. In the second stage, the recommended CS is optimized for ERVs that finished last ride-hailing order. According to the collected charging location and price information, the optimal CS decisions are made comprehensively considering the driving time, waiting time and charging cost. At this time, the platform releases the recommendation information to both the ERV and the building simultaneously. Upon arrival at the CS, ERVs begin charging via piles in/around the buildings to meet their energy-sharing requirement. The ERVs pay for the charging to the buildings to realize value transmission. Both of the energy and value transmission is ultimately achieved through the information interactions among the platform, ERVs and Passengers.

Module operation sequence. Within the urban mobility-energy sharing service framework, a key coupling exists between the mobility sharing and energy sharing services, as the PCG for energy sharing directly depends on the outcomes of mobility order matching. Furthermore, the updating CS information is dynamically influenced by both the PCG and the optimal station recommendation processes. To make the operation of four functional modules fluently, a standardized operational sequence is established, illustrated in Figure 1.

Building-side energy sharing mechanism. The core mechanism of the building-side energy sharing lies in guiding the spatial distribution of ERV charging loads through dynamic charging prices, thereby optimizing the operational efficiency of the building energy system. Specifically, the buildings accordingly set charging prices for their charging piles on the platform. These prices are determined based on real-time factors including internal renewable energy generation, distributed flexible energy resources, multi-energy load requirement, and the external power prices and carbon emission factors. Thus, the charging price from a building signal the internal energy production and consumption, as well as green value of charging at that location. By strategically reducing charging prices during periods of high renewable output, buildings can attract more ERV charging, thereby directly channeling electric vehicle demand to enhance the local consumption of renewable energy.

Two-stage charging guidance strategy

CS dynamic queue problem description. Based on the idea of simulation clock advancement in discrete-event systems, a three-layer queue model is formulated to simulate the dynamic queuing of CSs. This model divides the CS queue into reservation queue, waiting queue, and charging queue, as shown in Figure 2. The queues are updated dynamically through the progression of four types events in ERV CSs: CS reservation, arrival at the CS, start of charging, and end of charging.

Assuming the traffic road network contains K CSs, the set of CSs at time t is represented as $CS_t = \{cs_{1,t}, \cdots, cs_{k,t}, \cdots, cs_{K,t}\}$.The information of CSs mainly includes their location, the number of charging piles, and three-layer queue information. The information is defined using Equation (1).

$$cs_{k,t} = \{l_k, n_k, [M_k(t), N_k(t), G_k(t), q_k(t)]\} \tag{1}$$

Where, l_k denotes the location of CS k; n_k represents the number of charging piles at CS k; $M_k(t)$, $N_k(t)$, $G_k(t)$ indicates the number of ERVs in the reservation, waiting, charging queue at time t separately; $q_k(t)$ indicates the set of charging end times for all ERVs in the three-layer queue at time t (sorted in ascending order).

Requesting and reserving charging of ERVs is defined as Event R. Arriving at CS is defined as Event A. Starting charging is defined as Event J, and leaving CS is defined as Event L.

When an ERV submits a charging request and ultimately selects CS k, Event R is triggered, adding a new time node to its corresponding set. The arrival time is calculated based on the distance between the ERV and CS k, then updates Event A. Subsequently, Event J and L are updated according to waiting duration and charging duration. Therefore, the time sets of Event R, A, J and L at CS k are represented as follows.

$$H_k^R = \{T_{k,1}^r, T_{k,2}^r, \cdots\}, H_k^A = \{T_{k,1}^a, T_{k,2}^a, \cdots\} \tag{2,3}$$

$$H_k^J = \{T_{k,1}^j, T_{k,2}^j, \cdots\}, H_k^L = \{T_{k,1}^l, T_{k,2}^l, \cdots\} \tag{4,5}$$

Where, $T_{k,1}^r$ represents the time node corresponding to the ERV that first submits a charging request in the current CS queue. $T_{k,1}^a$ $T_{k,1}^j$ and $T_{k,1}^l$ respectively represent the time nodes corresponding to the ERV that first arrives, starts charging, and leaves the CS. By counting the time nodes of all four types of events that ERVs trigger, the time set T of all events is obtained.

$$T = H^R \cup H^A \cup H^J \cup H^L = \{T_1, T_2, \ldots, T_f, \ldots, T_F\} \tag{6}$$

For Charging CS k at each time node T_f in the time set T, define binary variables $W_k(T_f)$ to denote whether an ERV reserves CS k under the guidance of the station recommendation, as shown in (7). Besides, $X_k(T_f)$, $Y_k(T_f)$, $Z_k(T_f)$ separately represents whether an ERV arrives, starts charging, and leaves CS k or not, defined as (8-10).

$$W_k(T_f) = \begin{cases} 1, T_f \in H_k^R \\ 0, T_f \notin H_k^R \end{cases}, X_k(T_f) = \begin{cases} 1, T_f \in H_k^A \\ 0, T_f \notin H_k^A \end{cases} \tag{7,8}$$

$$Y_k(T_f) = \begin{cases} 1, T_f \in H_k^J \\ 0, T_f \notin H_k^J \end{cases}, Z_k(T_f) = \begin{cases} 1, T_f \in H_k^L \\ 0, T_f \notin H_k^L \end{cases} \tag{9,10}$$

The total queuing number of ERVs at time node T_f , defined with $S_k(T_f)$, is expressed as:

$$S_k(T_f) = M_k(T_f) + N_k(T_f) + G_k(T_f) \tag{11}$$

At time T_{f+1}, the moment when the next event occurs, the number of ERVs in each queue of CS k can be updated by Equation (12).

$$\begin{cases} M_k(T_{f+1}) = M_k(T_f) + W_k(T_f) - X_k(T_f) \\ N_k(T_{f+1}) = N_k(T_f) + X_k(T_f) - Y_k(T_f) \\ G_k(T_{f+1}) = G_k(T_f) + Y_k(T_f) - Z_k(T_f) \\ S_k(T_{f+1}) = S_k(T_f) + W_k(T_f) - Z_k(T_f) \end{cases} \tag{12}$$

Assuming PCG of ERV n is completed at time T_n^g, the time of ERV arrival at CS T_n^a can be calculated using (13):

$$T_n^a = T_n^g + \frac{dis\langle l_{n,t}, l_k \rangle}{\overline{V^{et}}} \tag{13}$$

Where, $dis\langle l_{n,t}, l_k\rangle$ denotes the shortest path length between the ERV's location $l_{n,t}$ and the CS's location l_k, calculated by the Dijkstra algorithm, $\overline{V^{et}}$ represents the average speed of the ERV on urban roads. Base on T_n^g and T_n^a, The time set H_k^R and H_k^A of Event R and A can be updated.

Furthermore, the charging end times of ERVs in the charging queue are sorted in ascending order. Specifically, by filtering time nodes where $T \geq T_n^a$ from the time set of Event L, a sorted charging end time set $q_k(T_n^a) = \{\widetilde{T_{k,1}}, \widetilde{T_{k,2}}, \cdots\}$ is constructed. Thus, the waiting time $t_{n,k}^w$ for ERVs can be calculated using (14).

$$t_{n,k}^w = \begin{cases} 0, N_k(T_n^a) + G_k(T_n^a) < n_k \\ q_k(T_n^a)[N_k(T_n^a) + G_k(T_n^a) - n_k + 1] - T_n^a, N_k(T_n^a) + G_k(T_n^a) \geq n_k \end{cases} \tag{14}$$

Where, $q_k(T^a)[x]$ denotes the x-th element in the charging end time set $q_k(T^a)$.

At this point, if a charging pile at CS k is damaged, update the number of available charging piles at CS k though $n_k = n_k - 1$. The calculation for charging duration $t_{n,k}^{ch}$ of ERVs is derived as (15).

$$t_{n,k}^{ch} = \frac{s_n^e E_n^{et} - E_n^a}{\eta_k^c P_k^c} \tag{15}$$

Where, s_n^e indicates the driver's desired SOC; E_n^{et} is the battery capacity of the ERV; E_n^a indicates the remaining battery capacity when ERV arrives at CS; η_k^c stands for charging efficiency; P_k^c denotes the charging power. Then, the time sets H_k^J and H_k^L for Events J and L need to be updated. As for the ERVs that complete CS reservations before n but arrive later, their corresponding elements in H_k^J and H_k^L should be modified, and the charging waiting time recalculated accordingly.

Pre-charging guidance strategy for ERVs. Define the information set of ERVs sending PCG requests at time t as $ET_t = \{et_{1,t}, \cdots, et_{n,t}, \cdots, et_{N,t}\}$, the travel order set of the passengers as $P_t = \{p_{1,t}, \cdots, p_{m,t}, \cdots, p_{M,t}\}$, queue information set of CS as $CS_t = \{cs_{1,t}, \cdots, cs_{k,t}, \cdots, cs_{K,t}\}$. The elements of these sets can be defined as (16)-(18).

$$et_{n,t} = \{l_{n,t}, s_{n,t}\} \tag{16}$$

$$p_{m,t} = \{o_{m,t}, d_{m,t}\} \tag{17}$$

$$cs_{k,t} = \{l_k, n_k, [M_k(t), N_k(t), G_k(t), q_k(t)]\} \tag{18}$$

Where, $l_{n,t}$ represents the location of ERV n at time t; $s_{n,t}$ denotes the SOC of ERV n; $o_{m,t}$ and $d_{m,t}$ are the origin and destination of passenger m's mobility order.

The PCG strategy for ERVs is generated via following steps.

Step 1: PCG request collection

When an ERV's SOC is close to the range anxiety threshold, PCG requests can be automatically generated and sent to the platform via terminal Application. At this point, upon receiving the request, the platform collects all the PCG requests within the time period [t-Δt, t] and processes them uniformly at time t. Based on the chronological order of PCG requests submitted by ERVs during the period [t-Δt, t], the platform sequentially executes the matchable order scanning and the optimal mobility order matching procedure.

Step 2: Screening of Pre-guidance matchable orders

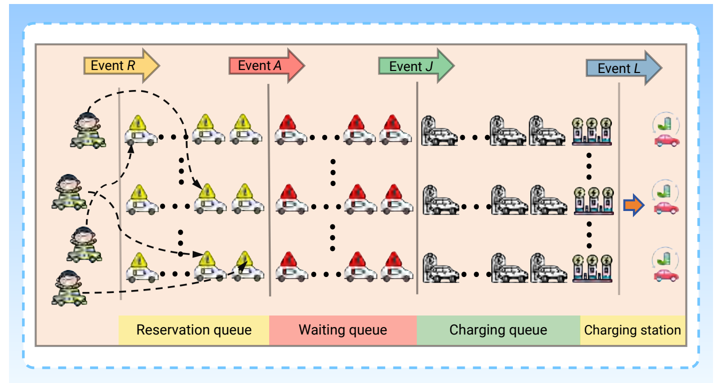

Figure 2. Three-layer dynamic queue model of CS

Taking ERV n participating in PCG as an example, ERVs that submitted PCG requests before ERV n during the time period [t-Δt, t] have completed optimal mobility order matching, and the matching results are assumed to be $MA_t = \{ma_{1,t}, \cdots, ma_{n-1,t}\}$. The platform needs to screen mobility orders that can meet the PCG requirements of the ERV based on the location and SOC information $et_{n,t}$, the origin and destination information P_t of the mobility order set, and the location information CS_t of the CSs. These orders are defined as pre-guidance matchable orders $P'_{n,t}$.

The screening process for pre-guidance matchable orders is listed as follows:

1) First, the platform conducts a primary screening on the mobility order set P_t based on the origin-destination pairs of each passenger, retaining mobility orders that meet the following conditions for ERV n:

$$\frac{dis\langle l_{n,t}, o_{m,t}\rangle}{\overline{V^{et}}} \leq t^{w,max} \tag{19}$$

Where, $dis\langle l_{n,t}, o_{m,t}\rangle$ represents the shortest path lengths between the location $l_{n,t}$ of ERV n at time t and the origin $o_{m,t}$ of passenger m's mobility, $t^{w,max}$ is the maximum acceptable waiting time for passengers.

2) For the mobility orders retained after the primary screening, a further screening is performed to verify whether ERV n can reach the nearest CS after order completion given its current SOC. This further screening retains mobility orders should meet (20).

$$\begin{aligned} s_{n,t}E_n^{et} - \Delta E_n^{et}(dis\langle l_{n,t}, o_{m,t}\rangle + dis\langle o_{m,t}, d_{m,t}\rangle \\ + min\{dis\langle d_{m,t}, l_k\rangle, k \in K\}) \geq s_n^{min} E_n^{et} \end{aligned} \tag{20}$$

Where, ΔE_n^{et} is the power consumption per kilometer of ERV n; s_n^{min} is the minimum acceptable SOC threshold for ERV drives.

3) Since each passenger can only be assigned to one ERV, the pre-guidance matchable orders of ERV n must not conflict with the mobility orders in the matching result $MA_t = \{ma_{1,t}, \cdots, ma_{n-1,t}\}$, thus completing the screening process.

Step 3: Optimal mobility order matching for ERVs under PCG

The optimal mobility order matching model is designed to simulate the charging selection behavior of ERV drivers under different matching schemes, and complete passenger-ERV matching with the goal of maximizing drivers' charging satisfaction.

Following the screening process, the set of matchable mobility orders for ERV $et_{n,t}$ is updated to $P'_{n,t} = \{p'_{1,t}, \cdots, p'_{m,t}, \cdots, p'_{M,t}\}$. The platform subsequently simulates the CS selection results of the ERV after completing the corresponding mobility orders under different matching schemes $ma_{n,t} \in P'_{n,t}$.

Taking the matching scheme $ma_{n,t} = p'_{m,t}$ as an example, the specific simulation process of charging selection behavior for ERV is organized as follows.

1) Under the matching scheme $ma_{n,t}$, the position and SOC of the ERV can be determined after completing the mobility order $p'_{m,t}$. Thus, the set of CSs accessible to ERV is identified. Combining the CS selection range with $et_{n,t}$, the candidate CS queue $csq_{n,m,t}$ is ultimately obtained.

$$csq_{n,m,t} = \{x_{n,m,1}, \cdots, x_{n,m,k}, \cdots, x_{n,m,K}\} \tag{21}$$

$$x_{n,m,k} = \begin{cases} 1, s_{n,t}E_n^{et} - \Delta E_n^{et}(dis\langle l_{n,t}, o_{m,t}\rangle + dis\langle o_{m,t}, d_{m,t}\rangle + dis\langle d_{m,t}, l_k\rangle) \geq s_n^{min}E_n^{et} \\ \text{and } dis\langle o_{m,t}, d_{m,t}\rangle \leq d^{cs,max} \\ 0, s_{n,t}E_n^{et} - \Delta E_n^{et}(dis\langle l_{n,t}, o_{m,t}\rangle + dis\langle o_{m,t}, d_{m,t}\rangle + dis\langle d_{m,t}, l_k\rangle) < s_n^{min}E_n^{et} \\ \text{and } dis\langle o_{m,t}, d_{m,t}\rangle > d^{cs,max} \end{cases} \tag{22}$$

Where, $x_{n,m,k}$ indicates whether the charging CS k is in the candidate CS queue of ERV n, if ERV can reach CS k, the value equals 1, else equals 0; $d^{cs,max}$ represents the CS search range of the ERV, i.e. the maximum acceptable distance to a CS.

2) Update of the selected queue $qcs_{k,t}$ for CS k based on the candidate CS queue $csq_{n,m,t}$ of ERV n. When the value of the k-th element in $csq_{n,m,t}$ equals to 1, CS k is a potential candidate for ERV n, then add the ERV n to the selected queue $qcs_{k,t}$ of the corresponding station based on the principle of $csq_{n,m,t}[k] = 1$. The specific update for the queue set $qcs_{k,t}$ is expressed as (23).

$$qcs_{k,t} \leftarrow \begin{cases} qcs_{k,t} \cup \{et_{n,t}\}, csq_{n,m,t}[k] = 1 \\ qcs_{k,t}, csq_{n,m,t}[k] = 0 \end{cases}, k \in K \tag{23}$$

3) Based on the selected queue of the CS and the queue information of the CS, the probability distribution of the queuing waiting time for the ERV n to select CS k can be obtained.

First, update the time sequence to the time t' when the ERV n completes the mobility order $p_{m,t}$ and arrives at the CS k with (24).

$$t' = t + \frac{dis\langle l_{n,t}, o_{m,t}\rangle + dis\langle o_{m,t}, d_{m,t}\rangle + dis\langle d_{m,t}, l_k\rangle}{V^{et}} \tag{24}$$

The queue waiting time $t_{n,k}^{w}$ can be directly calculated according to CS k's queue information $[M_k(t'), N_k(t'), G_k(t'), q_k(t')]$ at time t' and (14).

However, among the ERVs that have completed optimal mobility order matching, there is still a subset of ERVs in the PCG stage that have not yet made their final CS selection decision. The competitive relationships for charging service resources between these ERVs and ERV n persists, manifested primarily as follows: the charging selection behavior of such ERVs may alter the relative position of ERV n in the target station's selection queue, thereby affecting its charging waiting time. In this scenario, the charging selection behavior of ERV n becomes a decision-making process based on queuing risk.

To establish this ERV risk decision-making scenario, the candidate queue of CSs must first be reorganized based on the chronological order of ERVs' arrival in the queue $qcs_{k,t}$. This reorganized queue is referred to as the virtual queue $V_{k,t}$. Considering that CS's queuing system adopts the first-come-first-served principle, an ERV's position in the virtual queue is associated with the time sequence of its arrival at CS. Therefore, the queue $qcs_{k,t}$ is reorganized. For example, assume that the matched mobility orders for $et_{a,t}$ and $et_{b,t}$ are $p_{x,t}$ and $p_{y,t}$, respectively. When $et_{a,t}$ and $et_{b,t}$ satisfy (25), $et_{a,t}$ will be positioned ahead of $et_{b,t}$ in the queue $qcs_{k,t}$.

$$dis\langle l_{a,t}, o_{x,t}\rangle + dis\langle o_{x,t}, d_{x,t}\rangle + dis\langle d_{x,t}, l_k\rangle \leq dis\langle l_{b,t}, o_{y,t}\rangle + dis\langle o_{y,t}, d_{y,t}\rangle + dis\langle d_{y,t}, l_k\rangle \tag{25}$$

The virtual queue $V_{k,t}$ achieves the sorting of the ERVs' arrival sequence at CS k within the selected queue $qcs_{k,t}$. Furthermore, based on the position $V_{k,t}[et_{n,t}]$ of $et_{n,t}$ in the virtual queue $V_{k,t}$, the charging queue waiting time $t_{n,k}^{w}$ of $et_{n,t}$ can be obtained.

$$t_{n,k}^{w}(V_{k,t}[et_{n,t}]) = \begin{cases} 0 \quad , M_k(t') + N_k(t') + G_k(t') + V_{k,t}[et_{n,t}] - 1 < n_k \\ q_k(t')[M_k(t') + N_k(t') + G_k(t') + V_{k,t}[et_{n,t}] - n_k] - t' \\ \quad , M_k(t') + N_k(t') + G_k(t') + V_{k,t}[et_{n,t}] - 1 \geq n_k \end{cases} \tag{26}$$

For ERVs positioned ahead of $V_{k,t}[et_{n,t}]$ in virtual queue $V_{k,t}$, their decisions on whether to charge at CS k constitutes an uncertain event. After accounting for charging uncertainty, the probability distribution of $T_{n,k}^{w}$ can be expressed by (27)-(28).

$$T_{n,k}^{w} = \left\{t_{n,k}^{w}(1), p_{k,1}; \cdots; t_{n,k}^{w}(x), p_{k,x}; \cdots; t_{n,k}^{w}(V_{k,t}[et_{n,t}]), p_{k,V_{k,t}[et_{n,t}]}\right\} \tag{27}$$

$$p_{k,x} = \frac{C_{V_{k,t}[et_{n,t}]-1}^{x-1}}{2^{V_{k,t}[et_{n,t}]-1}} = \frac{\dfrac{(V_{k,t}[et_{n,t}]-1)!}{(x-1)!(V_{k,t}[et_{n,t}]-x)!}}{2^{V_{k,t}[et_{n,t}]-1}} \tag{28}$$

Where, $p_{k,x}$ represents the probability distribution of different queue waiting time for $et_{n,t}$.

4) Based on the probability distribution of $T_{n,k}^{w}$, the comprehensive charging cost $C_{n,k,t}$ of ERV in risk decision-making scenarios can be obtained using (29)-(31).

$$C_{n,k,t} = vot \sum_{x=1}^{V_{k,t}[et_{n,t}]} \left[t_{n,k}^{w}(x) + t_{n,k}^{r}\right] p_{k,x} + C_{n,k}^{ch} \tag{29}$$

$$t_{n,k}^{r} = \frac{dis\langle l_{n,t}, l_k\rangle}{V^{et}} \tag{30}$$

$$C_{n,k}^{ch} = \rho_{k,t} \frac{(s_n^e - s_{n,t})E_n^{et} + \Delta E_n^{et}(dis\langle l_{n,t}, o_{m,t}\rangle + dis\langle o_{m,t}, d_{m,t}\rangle + dis\langle d_{m,t}, l_k\rangle)}{\eta_k^c} \tag{31}$$

Where, vot is the time-value factor, representing the conversion between the time cost attributes and fee cost attributes; $C_{n,k}^{ch}$ is the fee that ERV n pay after completing the charging at CS k; $\rho_{k,t}$ represents the charging price at CS k at time t.

Finally, the ERV n will select the CS with the minimum comprehensive charging cost from the candidate CS queue $csq_{n,m,t}$.

$$\underset{k \in K, csq_{n,m,t}[k]=1}{argmin}[C_{n,k,t}] = \underset{k \in K, csq_{n,m,t}[k]=1}{argmin}\left[vot \sum_{x=1}^{V_{k,t}[et_{n,t}]}\left[t_{n,k}^{w}(x) + t_{n,k}^{r}\right]p_{k,x} + C_{n,k}^{ch}\right] \tag{32}$$

5) Furthermore, the optimal mobility order is determined from the matchable mobility orders $P'_{n,t} = \{p'_{1,t}, \cdots, p'_{m,t}, \cdots, p'_{M,t}\}$ for ERV n. The specific matching objective function is (33).

$$\min_{ma_{n,t} \in P'_{n,t}}\left[\underset{k \in K, csq_{n,m,t}[k]=1}{argmin} C_{n,k,t}\right] \tag{33}$$

Through Step 1 - Step 3, the PCG for ERVs based on mobility-sharing services ultimately is completed. The complete matching process for all ERVs in PCG stage within the time period [t-Δt, t] can be found in Figure S2.

Optimal CS recommendation decision-making for ERVs. The platform achieves the last mobility order's optimal matching for ERVs via PCG based on the mobility sharing service, effectively improving the charging satisfaction. To further optimize the charging experience of ERV drivers, an optimal CS recommendation service is introduced, i.e. the second stage of charging guidance. According to the real-time information of ERVs after completing the PCG mobility orders, the service recommends the CS with the minimum comprehensive charging cost from the candidate CS queue for drivers.

To ensure the decision-making accuracy of the optimal CS recommendation module, a CS queue update module is introduced to update the queue status based on four types of events: Event R, Event A, Event J, and Event L. The specific update methods for the three-layer dynamic queue and virtual queue of the CS when different types of events are triggered are as follows.

1) Upon completion of the PCG phase, the platform activates the optimal CS recommendation module for ERV $et_{n,t}$. Based on the recommendation result, the ERV $et_{n,t}$ submits a charging request to the corresponding CS k and join the charging reservation queue. This action triggers a charging request event R, and a corresponding time node t_n^r is added to the time set H_k^R. Furthermore, the CS reservation queue can be updated according to (7) and (12). Meanwhile, since the ERV has determined the CS selection, the CS k with $x_{n,m,k} = 1$ in the candidate CS queue $csq_{n,m,t}$ needs to synchronously update the status of the virtual queue $V_{k,t}$. The specific update method is as follows: remove the ERV $et_{n,t}$ from the virtual queues of these CSs.

2) After completing the updates of the charging reservation queue and the virtual queue, the platform plans the optimal route to the CS for the driver

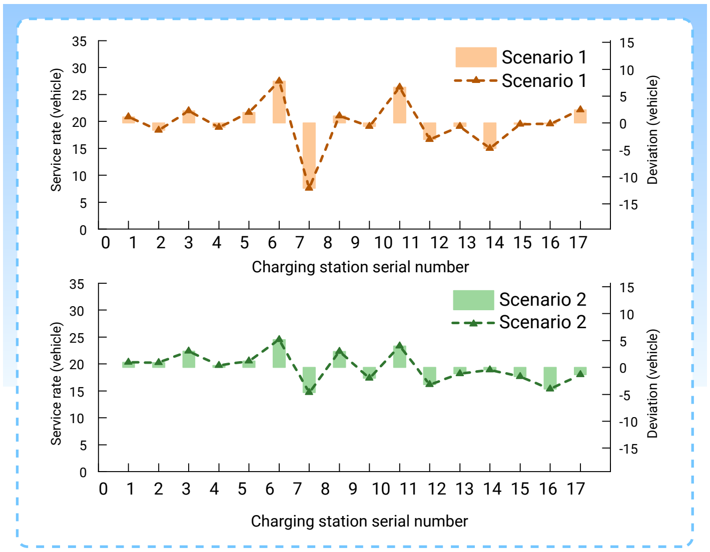

Figure 3. CS service rates and their deviations across two Scenarios

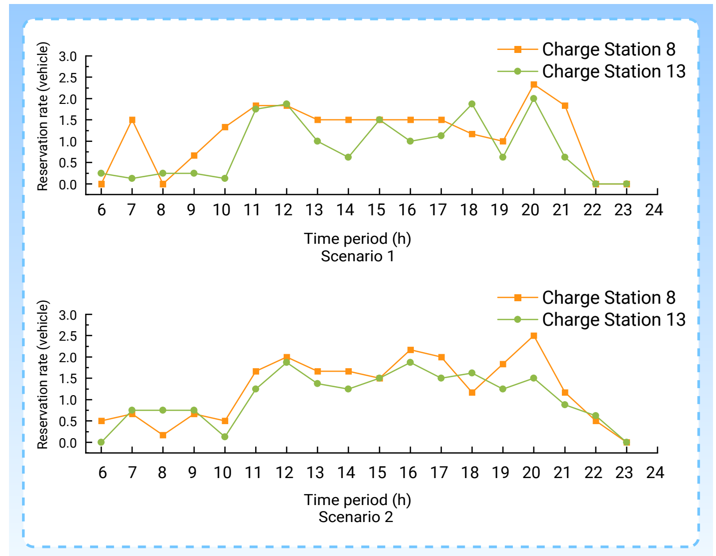

Figure 4. Comparison of reservation rates between central-area CS 8 and remote-area CS 13 in operation time period under two Scenarios

using Dijkstra's algorithm. When the ERV arrives at the CS, event A is triggered. The mobility time from the ERV's position to the CS can be calculated using (13), thereby determining the arrival time t_n^a, which is then added to the time H_k^A. As the simulation clock advances to t_n^a, the reservation queue and waiting queue of the CS are subsequently updated in accordance with (8) and (12).

3) At time t_n^a, the queue waiting time and charging duration for the ERV are calculated using Eq. (14) and (15) respectively, this enables the determination of two key time nodes: t_n^j when charging begins, and t_n^l when charging ends. When the simulation clock advances to t_n^j, event J is triggered, requiring updates to the station's waiting queue and charging queue according to (9) and (12). Subsequently, when the simulation clock advances to t_n^l, event L is triggered, necessitating a corresponding update to the charging queue based on Equations (10) and (12).

Based on real-time CS queues information, the optimal CS recommendation module screens the CS with the lowest comprehensive cost for ERVs. Assuming that ERV $et_{n,t}$ completes its PCG mobility order and activates the recommendation module at time t_n^e. At this moment, according to the CS queue and virtual queue information at time t_n^e, the CS selection risk scenario is reconstructed using Equations (27) -(28), ultimately yielding the objective function for the optimal CS recommendation is obtained.

$$\underset{k\in K, csq_{n,m,t_n^e}[k]=1}{argmin}\ [C_{n,k,t}] = \underset{k\in K, csq_{n,m,t_n^e}[k]=1}{argmin}\left[vot\sum_{x=1}^{V_{k,t_n^e}[et_{n,t}]}\left[t_{n,k}^w(x)+t_{n,k}^r\right]p_{k,x}+C_{n,k}^{ch}\right] \tag{34}$$

The optimal CS recommendation module activates an ERV event-tracking function after completing the CS recommendation for ERV. This function monitors vehicle charging events in real time and maintains information sharing with the CS queue update module. In turn, the queue update module dynamically adjusts station queue status based on the event data fed back from the recommendation module. This mechanism ensures that both the PCG module and the CS recommendation module always operate with accurate, up-to-date queue information, maintaining system-wide consistency in subsequent decision-making cycles.

RESULTS

Algorithm feasibility

This study developed the actual algorithm using the Python 3.9 programming language within the PyCharm IDE, and implemented it on a commercial computer equipped with 32GB RAM and an Intel(R) Core (TM) Ultra 9 275HX processor. The proposed strategy does not require real-time responses to ERV drivers. When drivers trigger range anxiety and submit PCG requests, they are typically still engaged in an ongoing order. During the period from the request submission until the completion of that order, the platform has sufficient time to match the driver with an optimal final mobility order. Therefore, even in high-demand scenarios, ample time remains for order matching. In the optimal CS recommendation phase, as uncertain parameters gradually converge to deterministic ranges, the computational complexity is not high. In summary, the strategy does not impose stringent requirements on the real-time performance of the algorithm.

Scenario setup

This study validates the effectiveness of the proposed urban mobility-energy sharing service framework using a real-world transportation network from a specific city, as detailed in supplementary note 3. To evaluate the efficacy of the two-stage charging guidance method for ERVs in guiding the spatial distribution of charging loads for ERVs and enhancing drivers' charging experience, two comparative scenarios are designed:

Scenario 1: The charging behavior of ERV drivers remains unguided. When charging is required, drivers search for accessible CSs within a 5 km radius and select the one with the lowest comprehensive charging cost, as determined by the station selection model (Equation S4).

Scenario 2: Drivers adopt two-stage charging guidance from the platform, and complete the charging process through PCG and optimal CS recommendation.

Analysis of service conditions for building CSs

Figure 3 compares the service rates and their deviations across CSs under Scenarios 1 and 2. Given the varying numbers of charging piles per station, the service rate, which reflects the average daily service volume per charging pile, is defined in this study as the ratio of the daily total number of ERVs serviced at a station to its number of charging piles. As shown in Figure 3, the service rate distribution in Scenario 1 is highly dispersed, with significant deviations from the mean and a variance of 27.35. This indicates that, without guidance for ERV charging behavior, concentrated demand leads to severe congestion at some stations while others remain underutilized, revealing an uneven distribution of resources. In contrast, Scenario 2 exhibits a more balanced service rate distribution with notably smaller deviations from the mean, reducing the variance to 13.96 and significantly improving utilization efficiency. A comprehensive analysis shows that the pre-guidance mechanism, which matches ERVs to CSs based on their last mobility order, effectively diverts traffic, disperses charging demand, and enhances overall station utilization. These results confirm the effectiveness of the proposed mechanism in optimizing the spatial allocation of ERV charging resources.

To visually demonstrate how the PCG mechanism optimizes the utilization balance across CSs, this paper analyzes two representative cases: CS 8, located in a central area, and CS 13, situated in a remote area. Figure 4 shows the reservation rates for the two CSs under Scenarios 1 and 2 over the service period. This rate is defined as the ratio of ERV reservations to charging piles per time period, to eliminate the influence of the difference in the

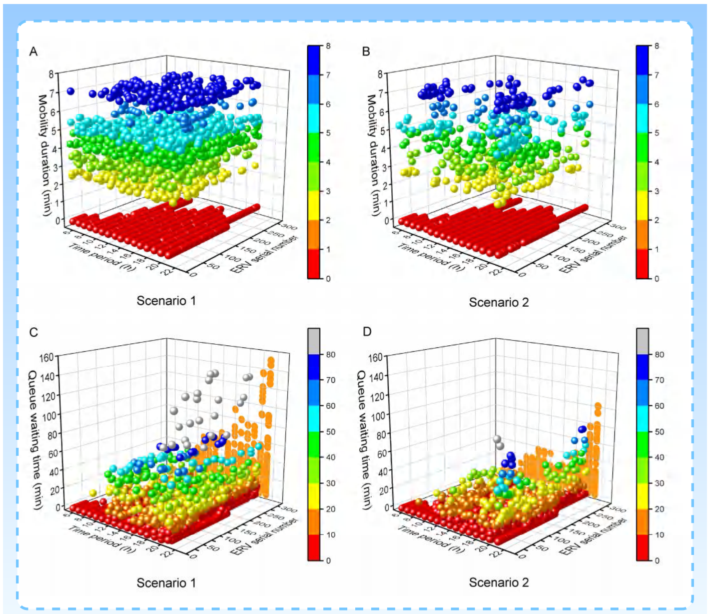

Figure 5. Mobility duration and queue waiting time of electric ride-hailing vehicles across two Scenarios. (A-B) Mobility duration distribution. (C-D) Queue waiting time distribution.

number of charging piles. In Scenario 1, CS 13 exhibits significantly lower reservation rates than Station 8 across most periods, constrained by its remote location. In Scenario 2, however, the PCG mechanism matches ERVs with mobility orders to remote areas, thereby directing them to underutilized peripheral stations. This results in a more balanced reservation rate between central and remote stations, demonstrating that the mechanism not only improves utilization balance but also helps prevent severe station congestion.

Analysis of charging satisfaction for ERV drivers

To quantify the impact of the PCG framework on ERV charging service satisfaction, this paper analyzes two key dimensions: the mobility duration to CSs and the queue waiting time at stations. By comparing these metrics between Scenarios 1 and 2, the extent to which the framework improves the charging experience can be systematically evaluated.

Figures 5A & B compare the mobility duration of ERVs to CSs under Scenarios 1 and 2. In Scenario 1, this duration is measured from the moment a charging demand is generated until station arrival. In Scenario 2, it is defined as the time between completing the PCG and reaching the station. Analysis reveals that, as the distance between network nodes typically exceeds 1.5 km, the mobility duration almost always surpasses 2 minutes, except when a demand arises exactly at a station. Notably, Scenario 2 shows a significant reduction in the number of ERVs with mobility times between 2-8 minutes. This indicates that the PCG effectively shortens mobility duration by matching ERVs with mobility orders destined for CSs.

The distribution of queue waiting times is presented in Figures 5C & D. As analyzed in Figure S5, a sustained peak in charging demand begins after 11:00. In Scenario 1, without the two-stage guidance, queue waiting times rise continuously, reaching up to 150 minutes. In contrast, Scenario 2, leveraging the PCG, distributes the demand evenly across stations via mobility order assignment. Consequently, despite increased demand, waiting times are largely contained within 60 minutes, effectively mitigating prolonged queuing and significantly improving the driver experience.

Complementing the preceding analysis of the mobility duration and the queue waiting time, Table 1 compares the average values of key ERV performance indicators under Scenarios 1 and 2.

As shown in Table 1, ERVs charging satisfaction demonstrate significant improvements in both time metrics. Specifically, compared to Scenario 1, during the charging process of ERVs, Scenario 2 achieves a 67.45% reduction in average mobility duration and a 50.73% decrease in average queue waiting time.

Table 1. Comparative analysis of charging satisfaction metrics for electric ride-hailing vehicles across scenarios

Scenario	Average mobility duration (min)	Average queue waiting time (min)	Average time Cost (RMB)	Average charging Cost (RMB)	Average total Cost (RMB)
Scenario1	2.7078	7.8221	3.8978	51.6280	55.5258
Scenario2	0.8813	3.8543	1.7530	50.6766	52.4296

CONCLUSION

This paper constructs an urban mobility-energy sharing service platform oriented towards passenger mobility sharing and proposes a two-stage charging guidance decision-making method, combining PCG with optimal CS recommendation. The PCG stage incorporates dynamic CS queues to model the probability distribution of waiting times, establishing a risk-aware decision-making framework. By matching ERVs with a final mobility order that minimizes their overall charging cost, this stage optimizes the spatial distribution of charging demand considering the regional building energy-sharing price. Subsequently, the CS recommendation stage synthesizes factors like mobility duration and queue waiting time to provide drivers with an optimal CS, thereby enhancing the charging experience and the energy sharing of nearby buildings. Simulation results demonstrate that, compared to an unguided charging mode, the proposed two-stage guidance under the platform significantly improves inter-station utilization balance and the charging experience for ERV drivers. This strategy offers an effective regulatory approach for integrating ERVs into building energy-sharing systems. More importantly, this study elucidates and validates a novel pathway for achieving V2B interactions by integrating mobility services with charging decision-making.

LIMINATIONS AND PERSPECTIVES

In this paper, the simulation assumes fixed vehicle models and charging times. However, with the rapid development of the new energy vehicle industry, real-world scenarios involve various types of ERVs. Moreover, as charging piles from different manufacturers have different output powers, charging durations also vary. In addition, under real-time pricing, the frequency of changes in charging costs increases significantly. Future research will further explore scenarios with different vehicle models, charging times, and pricing strategies.

While this study focuses on achieving a balanced spatial distribution of charging loads through ERV guidance, the optimization of temporal guidance and the development of spatiotemporal coordination mechanisms remain to be explored. Moreover, the current energy interaction framework only considers ERVs and buildings, without incorporating the power grid as a key stakeholder. Establishing a comprehensive energy interaction framework encompassing ERVs, buildings, and the power grid will be an important direction for future research.

REFERENCES

1. IEA (2023). Tracking Clean Energy Progress 2023, IEA, Paris. https://www.iea.org/reports/tracking-clean-energy-progress-2023
2. Chen X. (2024). Green and low-carbon energy-use. *Innov. Energy.* **1**:100003. DOI:10.59717/j.xinn-energy.2024.100003
3. Chen X., Liu J., Lin B., et al. (2025). Promote the Revolution in Energy Use to Enhance the Impetus for Green Transformation and Development. *Energy Use.* **1**:100001. DOI:10.59717/ipj.energy-use.2025.100001
4. Chen X. (2025). Energy-use Net: Path to Green and Low-carbon Energy-use. *Proceedings of the CSEE*, 1-18. https://link.cnki.net/urlid/11.2107.tm.20250909.1416.003.(in Chinese).
5. Wang Y., Ma M., Zhou N., et al. (2025). Paving the way to carbon neutrality: Evaluating the decarbonization of residential building electrification worldwide. *Sustain. Cities Soc.* **130**:106549. DOI:10.1016/j.scs.2025.106549
6. Liang Y., Yu C., and Pan W. (2025). Energy efficiency, renewables, and electrification contribute to decarbonising the operation of residential building stock in Hong Kong. *Energy Build.* **349**:116520. DOI:10.1016/j.enbuild.2025.116520
7. Yu J., Wang Q., Zhang X., et al. (2026). Optimizing photovoltaic energy sharing: A novel framework based on Stackelberg games in distribution networks. *Renew. Energy.* **256**:123870. DOI:10.1016/j.renene.2025.123870

8. Ivona Š., Mirna G., and Tomislav C. (2025). Energy sharing: Encouraging citizen participation in energy communities and collective self-consumption. *Energy.* **338**:138911. DOI:10.1016/j.energy.2025.138911
9. Kang J., Wang J., Liu C., et al. (2024). Coordinated optimization of configuration and operation of a photovoltaic integrated building cooling system with electricity and ice storages under source-load uncertainties. *Energy Build.* **320**:114600. DOI:10.1016/j.enbuild.2024.114600
10. Li G., Xu X., Cheng X., et al. (2025). Robust configuration planning for net zero-energy buildings considering source-load dual uncertainty and hybrid energy storage system. *Build. Environ.* **282**:113239. DOI:10.1016/j.buildenv.2025.113239
11. Wu Y., Liu Z., Li B., et al. (2025). Optimal storage capacity for building photovoltaic-energy storage systems considering energy flexibility management. *Energy Build.* **338**:115757. DOI:10.1016/j.enbuild.2025.115757
12. Li S., Chen X., Bu L., et al. (2024). Two-stage optimization for the air conditioning system in public buildings with flexible control of indoor load. *Energy Build.* **312**:114162. DOI:10.1016/j.enbuild.2024.114162
13. Wang M., Wang M., Wang R., et al. (2024). Optimization scheduling for low-carbon operation of building integrated energy systems considering source-load uncertainty and user comfort. *Energy Build.* **318**:114423. DOI:10.1016/j.enbuild.2024.114423
14. Yao Z., Ran L., Wang Z., et al. (2024). Integrated management of electric vehicle sharing system operations and Internet of Vehicles energy scheduling. *Energy.* **309**:132498. DOI:10.1016/j.energy.2024.132498
15. IEA (2025). Global EV Outlook 2025, IEA, Paris. https://www.iea.org/reports/global-ev-outlook-2025
16. María V., Jose C., Juan G., et al. (2025). Integrating shared mobility into multimodal habits: A comparative analysis across shared micro- and 'macro'-mobility services. *Transp. Policy.* **174**:103840. DOI:10.1016/j.tranpol.2025.103840
17. Gao F., Sylvia Y., Han C., et al. (2024). The impact of shared mobility on metro ridership: The non-linear effects of bike-sharing and ride-hailing services. *Travel Behav. Soc.* **37**:100842. DOI:10.1016/j.tbs.2024.100842
18. Morteza T., Samuel S., and Xu M. (2022). Widespread range suitability and cost competitiveness of electric vehicles for ride-hailing drivers. *Appl. Energy.* **319**:119246. DOI:10.1016/j.apenergy.2022.119246
19. Tang W., Chen X. (Michael), and Lee D-H. (2025). Toward mobility incentive: Integrating green service and carbon inclusion scheme into the ride-hailing market. *Transp. Res. B Methodol.* **201**:103320. DOI:10.1016/j.trb.2025.103320
20. Zhang Z., Yu Q., Gao K., et al. (2025). Carbon emission reduction benefits of ride-hailing vehicle electrification considering energy structure. *Appl. Energy.* **377**:124548. DOI:10.1016/j.apenergy.2024.124548
21. Li J., Xu X., Hamid R., et al. (2025). Optimization of electric vehicle charging strategies in residential integrated energy systems: A SARIMA model approach for dynamic electricity prices. *Energy.* **330**:136600. DOI:10.1016/j.energy.2025.136600
22. Wu H., Lan X., He Y., et al. (2025). Orderly charging of electric vehicles: A two-stage spatial-temporal scheduling method based on user-personalized navigation. *Appl. Energy.* **378**:124800. DOI:10.1016/j.apenergy.2024.124800
23. Liu G., Wang B., Li T., et al. (2025). Multi-objective electric-carbon synergy optimisation for electric vehicle charging: Integrating uncertainty and bounded rational behaviour models. *Appl. Energy.* **389**:125790. DOI:10.1016/j.apenergy.2025.125790
24. Chen X. (2025). Urban Energy Use and Its Friendly Interaction with Power Grid. *Energy Use.* **1**:100011. DOI:10.59717/ipj.energy-use.2025.100011
25. Abdalla M. A. A., Min W., Bing W., et al. (2023). Double-layer home energy management strategy for increasing PV self-consumption and cost reduction through appliances scheduling, EV, and storage. *Energy Rep.* **10**:3494-3518. DOI:10.1016/j.egyr.2023.10.019
26. Michele D., Tohid H., Anna R., et al. (2025). Enhancing voltage optimization in distribution networks through flexible operation of EV parking lots. *Sustain. Energy Grids Netw.* **41**:101601. DOI:10.1016/j.segan.2024.101601
27. Yan Q., Wang J., Lin T., et al. (2025). Peak-Valley difference based pricing strategy and optimization for PV-storage electric vehicle charging stations through ggregators. *Int. J. Electr. Power Energy Syst.* **169**:110812. DOI:10.1016/j.ijepes.2025.110812
28. Xiang Y., Yang J., Li X., et al. (2022). Routing optimization of electric vehicles for charging with event-driven pricing strategy. *IEEE Trans. Autom. Sci. Eng.* **19**:7–20. DOI:10.1109/tase.2021.3102997
29. Su S., Li Y., Yamashita K., et al. (2024). Electric vehicle charging guidance strategy considering "traffic network-charging station-driver" modeling: a multiagent deep reinforcement learning-based approach. *IEEE Trans. Transp. Electrific.* **10**:4653–4666. DOI:10.1109/tte.2023.3322685
30. Tao Y., Qiu J., Lai S., et al. (2024). Distributed electric vehicle assignment and charging navigation in cyber-physical systems. *IEEE Trans. Smart Grid.* **15**:1861–1875. DOI:10.1109/tsg.2023.3293251
31. Sun X., and Qiu J. (2021). Hierarchical voltage control strategy in distribution networks considering customized charging navigation of electric vehicles. *IEEE Trans. Smart Grid.* **12**:4752–4764. DOI:10.1109/tsg.2021.3094891
32. Habbal A., and Alrifaie M. F. (2024). A user-preference-based charging station recommendation for electric vehicles. *IEEE Trans. Intell. Transp. Syst.* **25**:11617–11634. DOI:10.1109/tits.2024.3379469
33. Yi Z., and Smart J. (2021). A framework for integrated dispatching and charging management of an autonomous electric vehicle ride-hailing fleet. *Transp. Res., Part D: Transp. Environ.* **95**:102822. DOI:10.1016/j.trd.2021.102822
34. Wang J., Cai H., Sun L., et al. (2025). MERCI: multi-agent reinforcement learning for enhancing on-demand electric taxi operation in terms of rebalancing, charging, and informing orders. *Comput. Ind. Eng.* **200**:110711. DOI:10.1016/j.cie.2024.110711
35. Li D., Hu C., Yang Q., et al. (2025). Charge or pick up. *Optimizing E-taxi management: a dual-stage heuristic coordinated reinforcement learning approach. IEEE Trans. Autom. Sci. Eng.* **22**:8533–8553. DOI:10.1109/tase.2024.3486342
36. Li X., Normandin-Taillon H., Wang C., et al. (2024). BM-RCWTSG: an integrated matching framework for electric vehicle ride-hailing services under stochastic guidance. *Sustain. Cities Soc.* **108**:105485. DOI:10.1016/j.scs.2024.105485
37. Zhong J., Liu J., and Zhang X. (2023). Charging navigation strategy for electric vehicles considering empty-loading ratio and dynamic electricity price. *Sustain. Energy Grids Netw.* **34**:100987. DOI:10.1016/j.segan.2022.100987
38. Ni W., Cheng P., Chen L., et al. (2024). Task assignment framework for online car-hailing systems with electric vehicles. *IEEE Trans. Knowl. Data Eng.* **36**:9361–9373. DOI:10.1109/tkde.2024.3434567
39. Patankar P. P., Hussain Rather Z., Liebman A., et al. (2025). Machine Learning-Based EV Charging Management System for Vehicle-to-Home and Vehicle-to-Building. *IEEE Trans. Transp. Electrific.* **11**:11100–11111. DOI:10.1109/tte.2025.3571793
40. Dai Y., Liu X., Li H., et al. (2025). Building-related electric vehicle charging behaviors and energy consumption patterns: An urban-scale analysis. *Transp. Res., Part D: Transp. Environ.* **141**:104663. DOI:10.1016/j.trd.2025.104663

FUNDING AND ACKNOWLEDGMENTS

This research was supported by the Shenzhen Science and Technology Program (KJZD20241122161901002) and the National Natural Science Foundation of China (Grant No. U22B20112 and No. 52207092).

AUTHOR CONTRIBUTIONS

All authors contributed to the manuscript and approved the final version.

DECLARATION OF INTERESTS

The authors declare no competing interests.

DATA AND CODE AVAILABILITY

Readers may contact the corresponding authors for data upon reasonable request.

SUPPLEMENTAL INFORMATION

It can be found online at https://doi.org/10.59717/ipj.energy-use.2025.100027